

Atmospheric Neutrino Oscillations, θ_{13} and Neutrino Mass Hierarchy

J. Bernabeu¹, Sergio Palmares-Ruiz¹ and S. T. Petcov²

¹ Departamento de Física Teórica and IFIC, Universidad de Valencia-CSIC, 46100 Burjassot, Valencia, Spain

² Scuola Internazionale Superiore di Studi Avanzati and Istituto Nazionale di Fisica Nucleare, I-34014 Trieste, Italy

Abstract

We derive predictions for the Nadir angle (θ_n) dependence of the ratio N_μ/N_e of the rates of the μ -like and e -like multi-GeV events measured in waterČerenkov detectors in the case of 3-neutrino oscillations of the atmospheric ν_e (ν_e) and ν_μ (ν_μ), driven by one neutrino mass squared difference, $\Delta m_{31}^2 \approx (2.5 - 3.0) \cdot 10^3 \text{ eV}^2 \approx m_{21}^2$. This ratio is particularly sensitive to the Earth matter effects in the atmospheric neutrino oscillations, and thus to the values of $\sin^2 \theta_{13}$ and $\sin^2 \theta_{23}$, θ_{13} and θ_{23} being the neutrino mixing angle limited by the CHOOZ and Palo Verde experiments and that responsible for the dominant atmospheric ν_μ (ν_μ) oscillations. It is also sensitive to the type of neutrino mass spectrum which can be with normal ($m_{31}^2 > 0$) or with inverted ($m_{31}^2 < 0$) hierarchy. We show that for $\sin^2 \theta_{13} > 0.01$, $\sin^2 \theta_{23} > 0.5$ and at $\cos \theta_n > 0.4$, the Earth matter effects modify substantially the θ_n dependence of the ratio N_μ/N_e and in a way which cannot be reproduced with $\sin^2 \theta_{13} = 0$ and a different value of $\sin^2 \theta_{23}$. For normal hierarchy the effects can be as large as 25% for $\cos \theta_n \in (0.5 - 0.8)$, can reach 35% in the Earth core bin $\cos \theta_n \in (0.84 - 1.0)$, and might be observable. They are typically by 10% smaller in the inverted hierarchy case. An observation of the Earth matter effects in the Nadir angle distribution of the ratio N_μ/N_e would clearly indicate that $\sin^2 \theta_{13} > 0.01$ and $\sin^2 \theta_{23} > 0.50$.

Also at: Institute of Nuclear Research and Nuclear Energy, Bulgarian Academy of Sciences, 1784 Sofia, Bulgaria.

1 Introduction

The publication of the first results of the KamLAND experiment marks the beginning of a new era in the studies of neutrino mixing and oscillations – the era of high precision determination of the neutrino mixing parameters. The data obtained by the solar neutrino experiments Homestake, Kamokande, SAGE, GALLEX/GNO and Super-Kamokande (SK) [1, 2] provided the first strong evidences for oscillations of flavour (electron) neutrinos. Strong evidences for oscillations of the atmospheric ($\bar{\nu}_\mu$) neutrinos were obtained by the Super-Kamokande (SK) experiment [3]. The evidences for solar ν_e oscillations into active neutrinos ν_μ, ν_τ , were significantly reinforced during the last two years i) by the combined first data of the SNO experiment [4], and the SK data [2], ii) by the more recent SNO neutral current data [5], and iii) by the first results of the KamLAND [6] experiment. The KamLAND data practically establishes [6], under the plausible assumption of CPT-invariance, the large mixing angle (LMA) MSW solution as unique solution of the solar neutrino problem. This result brings us, after more than 30 years of research, initiated by the pioneer works of B. Pontecorvo [7] and the experiment of R. Davis et al. [8], very close to a complete understanding of the true cause of the solar neutrino problem.

The interpretation of the solar and atmospheric neutrino, and of the KamLAND data in terms of neutrino oscillations requires the existence of 3-neutrino mixing in the weak charged lepton current (see, e.g., [9]):

$$\mathbb{L} = \sum_{j=1}^3 U_{lj} \nu_{jL} \quad (1)$$

Here $\mathbb{L}, l = e, \mu, \tau$, are the three left-handed flavour neutrino fields, ν_{jL} is the left-handed field of the neutrino ν_j having a mass m_j and U is the Pontecorvo-Maki-Nakagawa-Sakata (PMNS) neutrino mixing matrix [10],

$$U = \begin{pmatrix} U_{e1} & U_{e2} & U_{e3} \\ U_{\mu 1} & U_{\mu 2} & U_{\mu 3} \\ U_{\tau 1} & U_{\tau 2} & U_{\tau 3} \end{pmatrix} = \begin{pmatrix} C_{12}C_{13} & s_{12}C_{13} & s_{13}e^{-i\delta} \\ s_{23}C_{23} & c_{23}s_{23}s_{13}e^{i\delta} & s_{23}C_{23} \\ s_{12}s_{23} & c_{23}s_{23}s_{13}e^{i\delta} & c_{23}C_{23} \end{pmatrix} \quad (2)$$

where we have used a standard parametrization of U with the usual notations, $s_{ij} = \sin \theta_{ij}$, $c_{ij} = \cos \theta_{ij}$, and δ is the Dirac CP-violation phase¹. If we identify m_{21}^2 and m_{31}^2 with the neutrino mass squared differences which drive the solar and atmospheric neutrino oscillations, $m_{21}^2 = m_{21}^2 > 0$, $m_{A}^2 = m_{31}^2$, the data suggest that $|m_{31}^2| \approx m_{21}^2$. In this case θ_{12} and θ_{23} , represent the neutrino mixing angles responsible for the solar and atmospheric neutrino oscillations, $\theta_{12} = \theta_{12}$, $\theta_{23} = \theta_{23}$, while θ_{13} is the angle limited by the data from the CHOOZ and Palo Verde experiments [13, 14].

Combined $\nu_e \rightarrow \nu_\mu$ and $\nu_e \rightarrow \nu_\tau$ oscillation analyses of the solar neutrino and KamLAND [6] data, performed under the assumption of CPT-invariance which we will suppose to hold throughout this study, show [15, 16] that the data favor the LMA MSW solution with $m^2 = (6.9 - 7.3) \times 10^5 \text{ eV}^2$ and $\tan^2 \theta_{12} = (0.42 - 0.46)$. A second, statistically somewhat less favored LMA solution (LMA II) exists at [15, 16] $m^2 = 1.5$

¹We have not written explicitly the two possible Majorana CP-violation phases which do not enter into the expressions for the oscillation probabilities of interest [11] (see also [12]). We assume throughout this study $0 \leq \theta_{12}; \theta_{23}; \theta_{13} < \pi/2$.

10^{-4} eV^2 . The atmospheric neutrino data, as is well known, is best described [3] in terms of dominant ν_μ (ν_τ) oscillations with $\Delta m_{21}^2 = 2.5 \times 10^{-3} \text{ eV}^2$ and $\sin^2 2\theta_A = 1.0$. The 90% C.L. allowed intervals of values of the two-neutrino oscillation parameters found in [3] read $\Delta m_{21}^2 = (1.9 - 4.0) \times 10^{-3} \text{ eV}^2$ and $\sin^2 2\theta_A = (0.89 - 1.0)$. According to the more recent combined analysis of the data from the SK and K2K experiments [17], one has $\Delta m_{21}^2 = (2.7 - 0.4) \times 10^{-3} \text{ eV}^2$. We will often use in our analysis as illustrative the values $\Delta m_{21}^2 = 3.0 \times 10^{-3} \text{ eV}^2$ and $\sin^2 2\theta_A = 0.92; 1.0$. Let us note that the atmospheric neutrino and K2K data do not allow one to determine the signs of Δm_{21}^2 , and of $\cos 2\theta_A$ when $\sin^2 2\theta_A \neq 1.0$. This implies that in the case of 3-neutrino mixing one can have $m_{31}^2 > 0$ or $m_{31}^2 < 0$. The two possibilities correspond to two different types of neutrino mass spectrum: with normal hierarchy (NH), $m_1 < m_2 < m_3$, and with inverted hierarchy (IH), $m_3 < m_1 < m_2$. The fact that the sign of $\cos 2\theta_A$ is not determined when $\sin^2 2\theta_A \neq 1.0$ implies that when, e.g., $\sin^2 2\theta_A = \sin^2 2\theta_{23} = 0.92$, two values of $\sin^2 2\theta_{23}$ are possible, $\sin^2 2\theta_{23} = 0.64$ or 0.36 .

In what regards the mixing angle θ_{13} , a 3-oscillation analysis of the CHOOZ data [18] led to the conclusion that for $\Delta m^2 < 10^{-4} \text{ eV}^2$, the limits on $\sin^2 \theta_{13}$ practically coincide with those derived in the 2-oscillation analysis in [13]. A combined 3-oscillation analysis of the solar neutrino, CHOOZ and the KamLAND data, performed under the assumption of $\Delta m^2 = \Delta m_{21}^2$ (see, e.g., [9, 19]), showed [15] that $\sin^2 \theta_{13} < 0.05$ at 99.73% C.L. The authors of [15] found the best-fit value of $\sin^2 \theta_{13}$ to lie in the interval $\sin^2 \theta_{13} = (0.00 - 0.01)$.

Getting more precise information about the value of the mixing angle θ_{13} , determining the sign of Δm_{21}^2 , or the type of the neutrino mass spectrum (with normal or inverted hierarchy), and measuring the value of $\sin^2 2\theta_{23}$ with a higher precision is of fundamental importance for the progress in the studies of neutrino mixing.

The mixing angle θ_{13} , or the absolute value of the element U_{e3} of the PMNS matrix, $|U_{e3}| = \sin \theta_{13}$, plays a very important role in the phenomenology of the 3-neutrino oscillations. It drives the subdominant ν_μ (ν_τ) oscillations of the atmospheric (ν_μ) and ν_e (ν_e) [20, 21, 22]. The value of θ_{13} controls also the $\nu_\mu \rightarrow \nu_e$, $\nu_\tau \rightarrow \nu_e$, $\nu_e \rightarrow \nu_\mu$ and $\nu_e \rightarrow \nu_\tau$ transitions in the long baseline neutrino oscillation experiments (MINOS, CNGS), and in the widely discussed very long baseline neutrino oscillation experiments at neutrino factories (see, e.g., [23, 24, 25, 26]). The magnitude of the T-violating and CP-violating probabilities in neutrino oscillations is directly proportional to $\sin \theta_{13}$ (see, e.g., [27, 28, 29]). Thus, in the subdominant channels of interest to T- and CP-violation studies, the corresponding asymmetries become proportional to $\Delta m^2 = \sin \theta_{13}$ [29, 30]. The value of $\sin \theta_{13}$ is thus of prime importance.

If the neutrinos with definite mass are Majorana particles (see, e.g., [12]), the predicted value of the effective Majorana mass parameter in neutrinoless double beta decay depends strongly in the case of hierarchical neutrino mass spectrum on the value of $\sin^2 \theta_{13}$ (see, e.g., [31]).

The sign of Δm_{21}^2 determines, for instance, which of the transitions (e.g., of atmospheric neutrinos) $\nu_\mu \rightarrow \nu_e$ and $\nu_e \rightarrow \nu_\mu$, or $\nu_\tau \rightarrow \nu_e$ and $\nu_e \rightarrow \nu_\tau$, can be enhanced by the Earth matter effects [32, 33, 34]. The predictions for the neutrino effective Majorana mass in neutrinoless double beta decay depend critically on the type of the neutrino mass spectrum (normal or inverted hierarchical) [31, 35]. The knowledge of the value of θ_{13} and of the sign of $\Delta m_{21}^2 = \Delta m_{31}^2$ is crucial for the searches for the correct theory of neutrino masses and

mixing as well.

Somewhat better limits on $\sin^2 \theta_{13}$ than the existing one can be obtained in the MINOS experiment [36]. Various options are being currently discussed (experiments with θ -axis neutrino beams, more precise reactor antineutrino and long base-line experiments, etc., see, e.g., [37]) of how to improve by at least an order of magnitude, i.e., to values of $\theta < 0.005$ or smaller, the sensitivity to $\sin^2 \theta_{13}$. The sign of m_A^2 can be determined in very long base-line neutrino oscillation experiments at neutrino factories (see, e.g., [23, 24]), and, e.g., using combined data from long base-line oscillation experiments at the JHF facility and with θ -axis neutrino beams [38]. If the neutrinos with definite mass are Majorana particles, it can be determined by measuring the effective neutrino Majorana mass in neutrinoless double decay experiments [31, 35]. Under certain rather special conditions it might be determined also in experiments with reactor $\bar{\nu}_e$ [39].

In the present article we study possibilities to obtain information on the value of $\sin^2 \theta_{13}$ and on the sign of $m_A^2 = m_{31}^2$ using the atmospheric neutrino data, accumulated by the SK experiment, and more generally, that can be provided by future water-Cherenkov detectors, like UNO and Hyper-Kamiokande. We consider 3-neutrino oscillations of the atmospheric ν_μ, ν_τ, ν_e and $\bar{\nu}_e$ under the condition $m^2 = m_{21}^2 - |m_A^2| = |m_{31}^2|$, which is suggested to hold by the current solar and atmospheric neutrino data. Under the indicated condition, the expressions for the probabilities of $\nu_\mu \rightarrow \nu_e$ ($\bar{\nu}_\mu \rightarrow \bar{\nu}_e$) and $\nu_\tau \rightarrow \nu_e$ ($\bar{\nu}_\tau \rightarrow \bar{\nu}_e$) transitions contain $\sin^2 \theta_{23}$ as a factor, which determines their maximal values. Depending on the sign of m_{31}^2 , the Earth matter effects can resonantly enhance either the $\nu_\mu \rightarrow \nu_e$ and $\bar{\nu}_\mu \rightarrow \bar{\nu}_e$, or the $\nu_\tau \rightarrow \nu_e$ and $\bar{\nu}_\tau \rightarrow \bar{\nu}_e$ transitions if $\sin^2 \theta_{13} \neq 0$. The effects of the enhancement can be substantial for $\sin^2 \theta_{13} > 0.01$. They are larger in the multi-GeV ν_e -like and $\bar{\nu}_e$ -like samples of events and for atmospheric neutrinos with relatively large path length in the Earth, crossing deeply the mantle [25, 24] or the mantle and the core [20, 22, 40, 41, 42], i.e., for $\cos \theta_n > 0.4$, where θ_n is the Nadir angle characterizing the neutrino trajectory in the Earth.

The $\nu_\mu \rightarrow \nu_e$ ($\bar{\nu}_\mu \rightarrow \bar{\nu}_e$) and $\nu_\tau \rightarrow \nu_e$ ($\bar{\nu}_\tau \rightarrow \bar{\nu}_e$) transitions in the Earth lead to the reduction of the rate of the multi-GeV ν_e -like events and to the increase of the rate of the multi-GeV $\bar{\nu}_e$ -like events in the Super-Kamiokande (or any other water-Cherenkov) detector with respect to the case of absence of these transitions (see, e.g., [20, 21, 22, 41, 42]). Correspondingly, as observables which are sensitive to the Earth matter effects, and thus to the value of $\sin^2 \theta_{13}$ and the sign of m_{31}^2 , as well as to $\sin^2 \theta_{23}$, we consider the Nadir-angle distributions of the ratios $N^3 = N_e^3$ and $N_e^3 = N_e^0$, where N^3 and N_e^3 and are the multi-GeV ν_e -like and $\bar{\nu}_e$ -like numbers of events (or event rates) in the case of 3-oscillations of the atmospheric ν_μ, ν_τ, ν_e and $\bar{\nu}_e$, and N_e^0 is the number of $\bar{\nu}_e$ -like events in the case of absence of oscillations ($\sin^2 \theta_{13} = 0$). The ratio of the energy and Nadir angle integrated ν_e -like and $\bar{\nu}_e$ -like events, $N = N_e$, has been measured with a relatively high precision by the SK experiment [3]. The systematic uncertainty, in particular, in the Nadir angle dependence of the ratio $N = N_e$ can be smaller than those on the measured Nadir angle distributions of ν_e -like and $\bar{\nu}_e$ -like events, N and N_e .

We obtain predictions for the Nadir-angle distributions of $N^3 = N_e^3$ and of $N_e^3 = N_e^0$ both for neutrino mass spectra with normal ($m_{31}^2 > 0$) and inverted ($m_{31}^2 < 0$) hierarchy, $(N^3 = N_e^3)_{NH}$, $(N^3 = N_e^3)_{IH}$, $(N_e^3 = N_e^0)_{NH}$ and $(N_e^3 = N_e^0)_{IH}$, and for $\sin^2 \theta_{23} = 0.64; 0.50; 0.36$. We compare the latter with the predicted Nadir-angle distributions i) of the ratio $N = N_e$ for the case the 3-neutrino oscillations taking place in vacuum, $(N^3 = N_e^3)_{vac}$, and ii) of the

ratio $N^2 = N_e^0$, where N^2 is the predicted number of ν_e like events in the case of 2-neutrino ν_e and ν_μ oscillations of the atmospheric ν_e and ν_μ . Predictions for the different types of ratios indicated above of the suitably integrated Nadir angle distributions of the ν_e like and ν_μ like multi-GeV events are also given. Our results show, in particular, that for $\sin^2 2_{13} > 0.50$, $\sin^2 13 > 0.01$ and $m_{31}^2 > 0$, the effects of the Earth matter enhanced ν_e and ν_μ transitions of the atmospheric ν_e and ν_μ might be observable with the Super-Kamiokande detector. Conversely, if the indicated effects are indeed observed in the Super-Kamiokande experiment, that would suggest in turn that $\sin^2 13 > 0.01$, $\sin^2 23 > 0.50$ and that the neutrino mass spectrum is with normal hierarchy, $m_{31}^2 > 0$.

Let us note finally that the Earth matter effects have been widely investigated (for a recent detailed study see, e.g., ref. [43] which contains also a rather complete list of references to earlier work on the subject). However, the study of the magnitude of the Earth matter effects in the Nadir angle distribution of the ratio of the multi-GeV ν_e like and ν_μ like events, measured in water-Cherenkov detectors, performed here overlaps very little with the earlier investigations.

2 3- Oscillations of Atmospheric Neutrinos in the Earth

In the present Section we summarize the results on the oscillations of atmospheric neutrinos crossing the Earth, which we use in our analysis.

2.1 Preliminary Remarks

The ν_e (ν_μ) and ν_e (ν_μ) oscillations of atmospheric neutrinos should exist and their effects could be observable if genuine three-flavour-neutrino mixing takes place in vacuum, i.e., if $\sin^2 2_{13} \neq 0$, and if $\sin^2 2_{13}$ is sufficiently large [20] (see also, e.g., [21, 22, 41, 42]). Under the condition $|m_{31}^2| = |m_{21}^2|$, which the neutrino mass squared differences determined by the existing atmospheric and solar neutrino and KamLAND data satisfy, the relevant three-neutrino ν_e (ν_μ) and ν_e (ν_μ) transition probabilities reduce effectively to a two-neutrino transition probability [44], with m_{31}^2 and $\sin^2 2_{13} = 4|U_{e3}|^2(1 - |U_{e3}|^2)$ playing the role of the relevant two-neutrino oscillation parameters. Thus, searching for the effects of ν_e (ν_μ) and ν_e (ν_μ) transitions of atmospheric neutrinos, amplified by Earth matter effects, can provide unique information, in particular, about the magnitude of $\sin^2 13$.

As is not difficult to show using the results of [44], the 3-neutrino oscillation probabilities of interest for atmospheric ν_e , having energy E and crossing the Earth along a trajectory characterized by a Nadir angle θ_n , have the following form (see also, e.g., [22, 25]):

$$P_3(\nu_e \rightarrow \nu_e) = 1 - P_2; \quad (3)$$

$$P_3(\nu_e \rightarrow \nu_\mu) = P_3(\nu_\mu \rightarrow \nu_e) = s_{23}^2 P_2; \quad (4)$$

$$P_3(\nu_e \rightarrow \nu_\tau) = c_{23}^2 P_2; \quad (5)$$

$$P_3(\nu_\mu \rightarrow \nu_\mu) = 1 - \frac{4}{s_{23}^2} P_2 - 2c_{23}^2 s_{23}^2 \frac{1}{h} \text{Re}(e^{iA_2}(\nu_\mu \rightarrow \nu_\tau)); \quad (6)$$

$$P_3(\nu_\mu \rightarrow \nu_\tau) = 1 - P_3(\nu_\mu \rightarrow \nu_\mu) - P_3(\nu_\mu \rightarrow \nu_e); \quad (7)$$

Here $P_2 = P_2(m_{31}^2; 13; E; \theta_n)$ is the probability of two-neutrino oscillations in the Earth which coincides in form with, e.g., the two-neutrino $\nu_e \rightarrow \nu_\mu$ transition probability, $P_2(\nu_e \rightarrow \nu_\mu)$, but describes $\nu_e \rightarrow \nu_\tau$ transitions, where $\theta^0 = s_{23}^2 + c_{23}^2$ [44], and $A_2(\theta)$ A_2 are known phase and two-neutrino transition probability amplitude. Analytic expressions for P_2 , θ , and A_2 will be given later.

Using eqs. (3) – (7) it is not difficult to convince oneself that the fluxes of atmospheric ν_e , of energy E , which reach the detector after crossing the Earth along a given trajectory specified by the value of θ_n , $\nu_e(E; \theta_n)$, are given by the following expressions in the case of the three-neutrino oscillations under discussion [21, 22]:

$$\nu_e(E; \theta_n) = \nu_e^0 [1 + (s_{23}^2 r - 1) P_2]; \quad (8)$$

$$\nu_e(E; \theta_n) = \nu_e^0 [1 + s_{23}^4 [(s_{23}^2 r)^{-1} - 1] P_2 - 2c_{23}^2 s_{23}^2 \sin^2 \theta_n \operatorname{Re}(e^{i A_2(\theta)})]; \quad (9)$$

where $\nu_e^0 = \nu_e^{(0)}(E; \theta_n)$ is the $\nu_e^{(0)}$ flux in the absence of neutrino oscillations and

$$r = r(E; \theta_n) = \frac{\nu_e^0(E; \theta_z)}{\nu_e^0(E; \theta_n)}; \quad (10)$$

The interpretation of the SK atmospheric neutrino data in terms of $\nu_e \rightarrow \nu_\mu$ oscillations requires the parameter s_{23}^2 to lie approximately in the interval (0.30 – 0.70), with 0.5 being the statistically preferred value. For the predicted ratio $r(E; \theta_n)$ of the atmospheric and ν_e fluxes for i) the Earth core crossing and ii) only mantle crossing neutrinos, having trajectories for which $0.4 < \cos \theta_n < 1.0$, one has [45, 46, 47]: $r(E; \theta_z) = (2.0 - 2.5)$ for the neutrinos giving contribution to the sub-GeV samples of Super-K atmospheric events, and $r(E; \theta_n) = (2.6 - 4.5)$ for those giving the main contribution to the multi-GeV samples. If $s_{23}^2 = 0.5$ and $r(E; \theta_z) = 2.0$, we have $(s_{23}^2 r(E; \theta_z) - 1) = 0$ and the possible effects of the $\nu_e \rightarrow \nu_\mu$ and $\nu_e \rightarrow \nu_\tau$ transitions on the ν_e and ν_μ fluxes, and correspondingly on the sub-GeV e-like sample of events, would be strongly suppressed even if these transitions were maximally enhanced by the Earth matter effects. For the multi-GeV neutrinos we have $(s_{23}^2 r(E; \theta_z) - 1) > 0.3$ (0.9) for $s_{23}^2 = 0.5$ (0.7). The factor $(s_{23}^2 r(E; \theta_z) - 1)$, for instance, amplifies the effect of the $\nu_e \rightarrow \nu_\mu$ transitions in the e-like sample for $E > (5 - 6)$ GeV, for which $r(E; \theta_z) > 4$ [45, 46, 47].

The same conclusions are valid for the effects of oscillations on the fluxes of, and event rates due to, atmospheric antineutrinos: $\bar{\nu}_e$ and $\bar{\nu}_\mu$. Actually, the formulae for anti-neutrino fluxes and oscillation probabilities are analogous to those for neutrinos: they can be obtained formally from eqs. (3) – (10) by replacing the neutrino related quantities – probabilities, θ , $A_2(\theta)$ and fluxes, with the corresponding quantities for antineutrinos: $P_2(m_{31}^2; 13; E; \theta_n) \rightarrow P_2(m_{31}^2; 13; E; \theta_n)$, $\theta \rightarrow \theta$, $A_2(\theta) \rightarrow A_2(\theta)$, $A_2 \rightarrow A_2$, $P_3(\nu_\mu \rightarrow \nu_\tau) \rightarrow P_3(\nu_\mu \rightarrow \nu_\tau)$, $\nu_e^{(0)}(E; \theta_n) \rightarrow \nu_e^{(0)}(E; \theta_n)$ and $r(E; \theta_n) \rightarrow r(E; \theta_n)$.

Equations (3) – (6), (8) – (9) and the similar equations for antineutrinos imply that in the case under study the effects of the $\nu_e \rightarrow \nu_\mu$, $\nu_e \rightarrow \nu_\tau$, and $\nu_e \rightarrow \nu_\tau$, $\nu_e \rightarrow \nu_\mu$ oscillations i) increase with the increase of s_{23}^2 and are maximal for the largest allowed value of s_{23}^2 , ii) should be considerably larger in the multi-GeV samples of events than in the sub-GeV samples, iii) in the case of the multi-GeV samples, they lead to an increase of the rate of e-like events and to a slight decrease of the ν_e -like event rate. This discussion suggests that

the quantity most sensitive to the effects of the oscillations of interest should be the ratio of the μ -like and e -like multi-GeV events (or event rates), $N_\mu = N_e$.

The magnitude of the effects we are interested in depends also on the 2-neutrino oscillation probabilities, $P_{21}(\theta_{13}; E; \nu_n)$ and $P_{22}(\theta_{13}; E; \nu_n)$. In the case of oscillations in vacuum we have $P_{21}(\theta_{13}; E; \nu_n) = P_{22}(\theta_{13}; E; \nu_n) = \sin^2 2\theta_{13}$. Given the existing limits on $\sin^2 2\theta_{13}$, the probabilities P_{21} and P_{22} cannot be large if the oscillations take place in vacuum. However, P_{21} or P_{22} can be strongly enhanced by the Earth matter effects. The latter depend on the Earth density profile and we will discuss it next briefly.

2.2 The Earth Model and the Two-Layer Density Approximation

As is well known, the Earth density distribution in the existing Earth models is assumed to be spherically symmetric² and there are two major density structures – the core and the mantle, and a certain number of substructures (shells or layers). The core radius and the depth of the mantle are known with a rather good precision and these data are incorporated in the Earth models. According to the Stacey 1977 and the more recent PREM models [48, 49], which are widely used in the calculations of the probabilities of neutrino oscillations in the Earth, the core has a radius $R_c = 3485.7$ km, the Earth mantle depth is approximately $R_{man} = 2885.3$ km, and the Earth radius is $R = 6371$ km. The mean values of the matter densities of the core and of the mantle read, respectively: $\rho_c = 11.5$ g/cm³ and $\rho_{man} = 4.5$ g/cm³.

All the interesting features of the atmospheric neutrino oscillations in the Earth can be understood quantitatively in the framework of the two-layer model of the Earth density distribution [20]. The density profile of the Earth in the two-layer model is assumed to consist of two structures – the mantle and the core, having different densities, ρ_{man} and ρ_c , and different electron fraction numbers, Y_e^{man} and Y_e^c , none of which however vary within a given structure. The densities ρ_{man} and ρ_c in the case of interest should be considered as mean effective densities along the neutrino trajectories, and they vary somewhat with the change of the trajectory [20]: $\rho_{man} = \rho_{man}$ and $\rho_c = \rho_c$. In the PREM and Stacey models one has for $\cos \theta_n > 0.4$: $\rho_{man} = (4 - 5)$ g/cm³ and $\rho_c = (11 - 12)$ g/cm³. For the electron fraction numbers in the mantle and in the core³ one can use the standard values [50] $Y_e^{man} = 0.49$ and $Y_e^c = 0.467$. Numerical calculations show [51] (see also [20, 27]) that, e.g., the $\nu_e \rightarrow \nu_\mu$ oscillation probability of interest, calculated within the two-layer model of the Earth with ρ_{man} and ρ_c for a given neutrino trajectory determined using the PREM (or the Stacey) model, reproduces with a remarkably high precision the corresponding probability calculated by solving numerically the relevant system of evolution equations with the much more sophisticated Earth density profile of the PREM (or Stacey) model.

We give below the expressions for the probability $P_{21}(E; \nu_n; \theta_{13})$, for the phase and for the amplitude $A_{21}(\theta_{13})$ in the two-layer approximation of the Earth density distribution and in the general case of neutrinos crossing the Earth core. The expression for $P_{22}(E; \nu_n; \theta_{13})$, as we have already indicated, coincides with that for the probability

²Let us note that because of the approximate spherical symmetry of the Earth, a given neutrino trajectory through the Earth is completely specified by its Nadir angle.

³The electron fraction number is given by $Y_e = N_e / (N_p + N_n) = N_p / (N_p + N_n)$, where N_e , N_p and N_n are the electron, proton and neutron number densities in matter, respectively.

of the two-neutrino $\nu_e - \nu_e$ transitions and has the form [20]⁴:

$$\begin{aligned}
 P_2(E; z; m_{31}^2; \theta_{13}) = & \frac{1}{2} [1 - \cos E^{\text{m an}} X^{\text{m an}}] \sin^2 2\theta_m^{\text{m an}} \\
 & + \frac{1}{4} [1 - \cos E^{\text{m an}} X^{\text{m an}}] [1 - \cos E^{\text{core}} X^{\text{core}}] \sin^2 (2\theta_m^{\text{m an}} - 4\theta_m^{\text{core}}) \sin^2 2\theta_m^{\text{core}} \\
 & + \frac{1}{4} [1 - \cos E^{\text{m an}} X^{\text{m an}}] [1 - \cos 2E^{\text{core}} X^{\text{core}}] \sin^2 2\theta_m^{\text{core}} \cos^2 (2\theta_m^{\text{m an}} - 2\theta_m^{\text{core}}) \\
 & + \frac{1}{4} [1 + \cos E^{\text{m an}} X^{\text{m an}}] [1 - \cos 2E^{\text{core}} X^{\text{core}}] \sin^2 2\theta_m^{\text{core}} \\
 & + \frac{1}{2} \sin E^{\text{m an}} X^{\text{m an}} \sin 2E^{\text{core}} X^{\text{core}} \sin^2 2\theta_m^{\text{core}} \cos (2\theta_m^{\text{m an}} - 2\theta_m^{\text{core}}) \\
 & + \frac{1}{4} [\cos (E^{\text{core}} X^{\text{core}} - E^{\text{m an}} X^{\text{m an}}) - \cos (E^{\text{core}} X^{\text{core}} + E^{\text{m an}} X^{\text{m an}})] \sin 4\theta_m^{\text{core}} \sin (2\theta_m^{\text{m an}} - 2\theta_m^{\text{core}}); \quad (11)
 \end{aligned}$$

Here

$$E^{\text{core}} (E^{\text{m an}}) = \frac{m_{31}^2}{2E} \left[1 - \frac{m_{\text{an}}^{\text{res}}(c)A}{m_{\text{an}}^{\text{res}}(c)} \cos^2 2\theta_{13} + \sin^2 2\theta_{13} \right]; \quad (12)$$

is the difference between the energies of the two energy-eigenstate neutrinos in the mantle (core), $\theta_m^{\text{m an}}$ and θ_m^{core} are the mixing angles in matter in the mantle and in the core, respectively,

$$\sin^2 2\theta_m^{\text{core}} (\sin^2 2\theta_m^{\text{m an}}) = \frac{\sin^2 2\theta_{13}}{(1 - \frac{m_{\text{an}}^{\text{res}}(c)}{m_{\text{an}}^{\text{res}}})^2 \cos^2 2\theta_{13} + \sin^2 2\theta_{13}}; \quad (13)$$

X^{core} is half of the distance the neutrino travels in the mantle and $X^{\text{m an}}$ is the length of the path of the neutrino in the core, $\rho_{\text{m an}}^{\text{res}}$ and ρ_c^{res} are the resonance densities in the mantle and in the core, and $\rho_{\text{m an}}$ and ρ_c are the mean densities along the neutrino trajectory in the mantle and in the core. For a neutrino trajectory which is specified by a given Nadir angle θ_n we have:

$$X^{\text{core}} = R \cos \theta_n \frac{q}{R_c^2 - R^2 \sin^2 \theta_n}; \quad X^{\text{m an}} = 2 \frac{q}{R_c^2 - R^2 \sin^2 \theta_n}; \quad (14)$$

where $R = 6371$ km is the Earth radius (in the PREM [49] and Stacey [48] models) and $R_c = 3485.7$ km is the core radius. The neutrinos cross the Earth core on the way to the detector for $\theta_n < 33.17^\circ$.

The resonance densities in the mantle and in the core can be obtained from the expressions

$$\rho_{\text{res}} = \frac{m_{31}^2 \cos 2\theta_{13}}{2E} \frac{1}{2G_F Y_e} m_N; \quad (15)$$

m_N being the nucleon mass, by using the specific values of Y_e in the mantle and in the core. We have $\rho_{\text{m an}}^{\text{res}} \ll \rho_c^{\text{res}}$ because $Y_e^c = 0.467$ and $Y_e^{\text{m an}} = 0.49$ [50] (see also [52]). Obviously, $Y_e^c \rho_c^{\text{res}} = Y_e^{\text{m an}} \rho_{\text{m an}}^{\text{res}}$.

⁴The expression for P_2 (eq. (11)) can be obtained from the expression for the probability $P_{e2} = P(\nu_e \rightarrow \nu_e)$ given in eq. (7) in [20] by formally setting $\theta = 0$ while keeping $\theta_m^{\text{core}} \neq 0$ and $\theta_m^{\text{m an}} \neq 0$.

The phase δ and the probability amplitude A_2 which appear in eq. (9) for the flux of atmospheric neutrinos in the case of three-flavour neutrino mixing and hierarchy between the neutrino mass squared differences and therefore can play an important role in the interpretation of the, e.g., Super-Kamiokande atmospheric neutrino data, have the following form in the two-layer model of the Earth density distribution [20, 21, 22]:

$$= \frac{1}{2} \left[\frac{m_{31}^2}{2E} X + \frac{P_{21}}{2G_F} \frac{1}{m_N} (X^0 Y_e^c + 2X^0 Y_e^{man}) - 2E^0 X^0 - E^0 X^0 \right] \frac{m_{21}^2}{2E} X \cos 2\theta_{12}; \quad (16)$$

$$A_2(\delta) = 1 + e^{i2E^0 X^0} \frac{h}{1} + e^{iE^0 X^0} \frac{1}{1} \cos^2(\theta_m^0) \cos^2(\theta_m^0) + e^{iE^0 X^0} \frac{1}{2} \cos^2(\theta_m^0) + \frac{1}{2} e^{iE^0 X^0} \frac{1}{1} e^{iE^0 X^0} \frac{1}{1} \sin(2\theta_m^0) \sin(2\theta_m^0); \quad (17)$$

where $X^0 = X^0 + 2X^0$.

The expressions for P_2 , and $A_2(\delta)$ can be obtained from the corresponding expressions for neutrinos by replacing $(m_{an})_{\nu}$ with $(-m_{an})_{\nu}$ in eqs. (12) and (13).

2.3 Oscillations in the Earth Mantle

In the two-layer model, the oscillations of atmospheric neutrinos crossing only the Earth mantle (but not the Earth core), correspond to oscillations in matter with constant density. The relevant expressions for P_2 , and $A_2(\delta)$ follow from eqs. (11), (16) and (17) by setting $X^0 = 0$ and using $X^0 = R \cos \theta_n$. The expressions for P_2 (P_2) and A_2 (A_2) have the standard well-known form.

In the case under study θ_{13} plays the role of a two-neutrino vacuum mixing angle in the probabilities P_2 and P_2 . Since $\sin^2 \theta_{13} < 0.05$, we have $\cos 2\theta_{13} > 0$. Consequently, the Earth matter effects can resonantly enhance P_2 for $m_{31}^2 > 0$ and P_2 if $m_{31}^2 < 0$ [25]. Due to the difference of cross sections for neutrinos and antineutrinos, approximately 2/3 of the total rate of the μ -like and e -like multi-GeV atmospheric neutrino events in the SK (and in any other water-Cherenkov) detector, i.e., $2N_\mu=3$ and $2N_e=3$, are due to neutrinos and $\bar{\nu}_e$, respectively, while the remaining $1=3$ of the multi-GeV event rates, i.e., $N_\mu=3$ and $N_e=3$, are produced by antineutrinos $\bar{\nu}_\mu$ and $\bar{\nu}_e$. This implies that the Earth matter effects in the multi-GeV samples of μ -like and e -like events will be larger if $m_{31}^2 > 0$, i.e., if the neutrino mass spectrum is with normal hierarchy, than if $m_{31}^2 < 0$ and the spectrum is with inverted hierarchy. Thus, the ratio N_μ/N_e of the multi-GeV μ -like and e -like event rates measured in the SK experiment is sensitive, in principle, to the type of the neutrino mass spectrum.

Consider for definiteness the case of $m_{31}^2 > 0$. It follows from eqs. (8) and (9) that the oscillation effects of interest will be maximal if $P_2 = 1$. The latter is possible provided i) the well-known resonance condition [33, 34], leading to $\sin^2 2\theta_m^0 = 1$, is fulfilled, and ii) $\cos 2E^0 X^0 = 1$. Given the values of m_{an} and Y_e^{man} , the first condition determines the neutrino energy at which P_2 can be enhanced:

$$E_{res} = 6.6 \frac{m_{31}^2 [10^3 \text{ eV}^2]}{(N_e^{man} N_A \text{ cm}^{-3})} \cos 2\theta_{13} \text{ GeV}; \quad (18)$$

⁵One can get the expression for the amplitude $A_2(\delta)$ from eq. (1) in ref. [20] by formally setting $\delta = \pi/2$ while keeping θ_m^0 and θ_m^0 arbitrary, and then interchanging $\sin \theta_m^0$ ($\sin \theta_m^0$) and $\cos \theta_m^0$ ($\cos \theta_m^0$).

where the signs are correlated and $\cos^2 \theta_{m1} \cos^2 \theta_{m2} \approx 0$. As was shown in [41], conditions (20) are fulfilled for the $\nu_e \rightarrow \nu_e$ and $\nu_e \rightarrow \nu_\mu$ transitions of the Earth core-crossing atmospheric neutrinos. A rather complete set of values of $m_{31}^2 = E$ and $\sin^2 2\theta_{13}$ for which both conditions in (20) hold and $P_2 = 1$ for neutrino trajectories with Nadir angle $\theta_n = 0; 13^\circ; 23^\circ; 30^\circ$ was also found in [41].

For $\sin^2 2\theta_{13} < 0.05$, there are two sets of values of m_{31}^2 and $\sin^2 2\theta_{13}$ for which eq. (20) is fulfilled and $P_2 = 1$. These two solutions of eq. (20) occur for, e.g., $\theta_n = 0; 13^\circ; 23^\circ$, at 1) $\sin^2 2\theta_{13} = 0.034; 0.039; 0.051$, $m_{31}^2 = E = 7.2; 7.0; 6.5 \cdot 10^7 \text{ eV}^2 = M \text{ eV}$, and at 2) $\sin^2 2\theta_{13} = 0.15; 0.17; 0.22$, $m_{31}^2 = E = 4.8; 4.5; 3.8 \cdot 10^7 \text{ eV}^2 = M \text{ eV}$ (see Table 2 in ref. [41]). The first solution corresponds to $\cos^2 \theta_{12} = 1$, $\cos^2 \theta_{13} = 1$ and $\sin^2(\theta_{m1}^2 - \theta_{m2}^2) = 1$. For $m^2 = 3 \cdot 10^3 \text{ eV}^2$, the total neutrino conversion occurs in the case of the first solution at $E = (4.2 - 4.7) \text{ GeV}$. The atmospheric ν_e and ν_μ with these energies contribute to the multi-GeV samples of ν_e like and ν_μ like events in the SK experiment. The values of $\sin^2 2\theta_{13}$ at which the second solution takes place are marginally allowed. If $m^2 = 3 \cdot 10^3 \text{ eV}^2$, one has $P_2 = 1$ for this solution for a given θ_n in the interval $0 < \theta_n < 23^\circ$ at E lying in the interval $E = (6.3 - 8.0) \text{ GeV}$.

The above discussion suggests, in particular, that the effects of the mantle-core (NOLR) enhancement of P_2 (or P_2) in the ratios $N_\mu = N_e$ and $N_e^3 = N_e^0$ increase rapidly with $\sin^2 2\theta_{13}$ as long as $\sin^2 2\theta_{13} < 0.01$, and should exhibit a rather weak dependence on $\sin^2 2\theta_{13}$ for $0.01 < \sin^2 2\theta_{13} < 0.05$. If 3-neutrino oscillations of atmospheric neutrinos take place, the magnitude of the matter effects in the multi-GeV ν_e like and ν_μ like event samples, produced by neutrinos crossing the Earth mantle (but not the core), should be larger than in the event samples due to neutrinos crossing only the Earth mantle (but not the core). This is a consequence of the fact that in the energy range of interest the atmospheric neutrino fluxes decrease rather rapidly with energy – approximately as $E^{-2.7}$, while the neutrino interaction cross section rises only linearly with E , and that the maximum of P_2 (or P_2) due to the NOLR takes place at approximately two times smaller energies than that due to the MSW effect for neutrinos crossing only the Earth mantle (e.g., at $E = (4.2 - 4.7) \text{ GeV}$ and $E = 10 \text{ GeV}$, respectively, for $m^2 = 3 \cdot 10^3 \text{ eV}^2$).

3 Results

The results of our analysis are summarized graphically in Figs. 1–5. We have used in the calculations the predictions for the Nadir angle and energy distributions of the atmospheric neutrino fluxes given in [47]. In this analysis, we only consider Deep Inelastic Scattering (DIS) cross sections and we make use of the GRV94 parton distributions given in [53].

The predicted dependences on $\cos \theta_n$ of the ratios of the multi-GeV ν_e like events (or event rates), integrated over the neutrino energy from the interval $E = (2.0 - 10.0) \text{ GeV}$, in the case i) of two-neutrino $\nu_e \rightarrow \nu_e$ and $\nu_e \rightarrow \nu_\mu$ oscillations in vacuum and no ν_e and ν_μ oscillations, $N^2 = N_e^0$, ii) three-neutrino oscillations in vacuum of $\nu_e \rightarrow \nu_e$, $\nu_e \rightarrow \nu_\mu$, $\nu_e \rightarrow \nu_\tau$ and $\nu_e \rightarrow \nu_\tau$, ($N^3 = N_e^3$)_{vac}, iii) three-neutrino oscillations of $\nu_e \rightarrow \nu_e$, $\nu_e \rightarrow \nu_\mu$, $\nu_e \rightarrow \nu_\tau$ and $\nu_e \rightarrow \nu_\tau$ in the Earth in the cases of neutrino mass spectrum with normal hierarchy ($N^3 = N_e^3$)_{NH}, and with inverted hierarchy,

⁶The term "neutrino oscillation length resonance" (NOLR) was used in [20] to denote the mantle-core enhancement effect in this case.

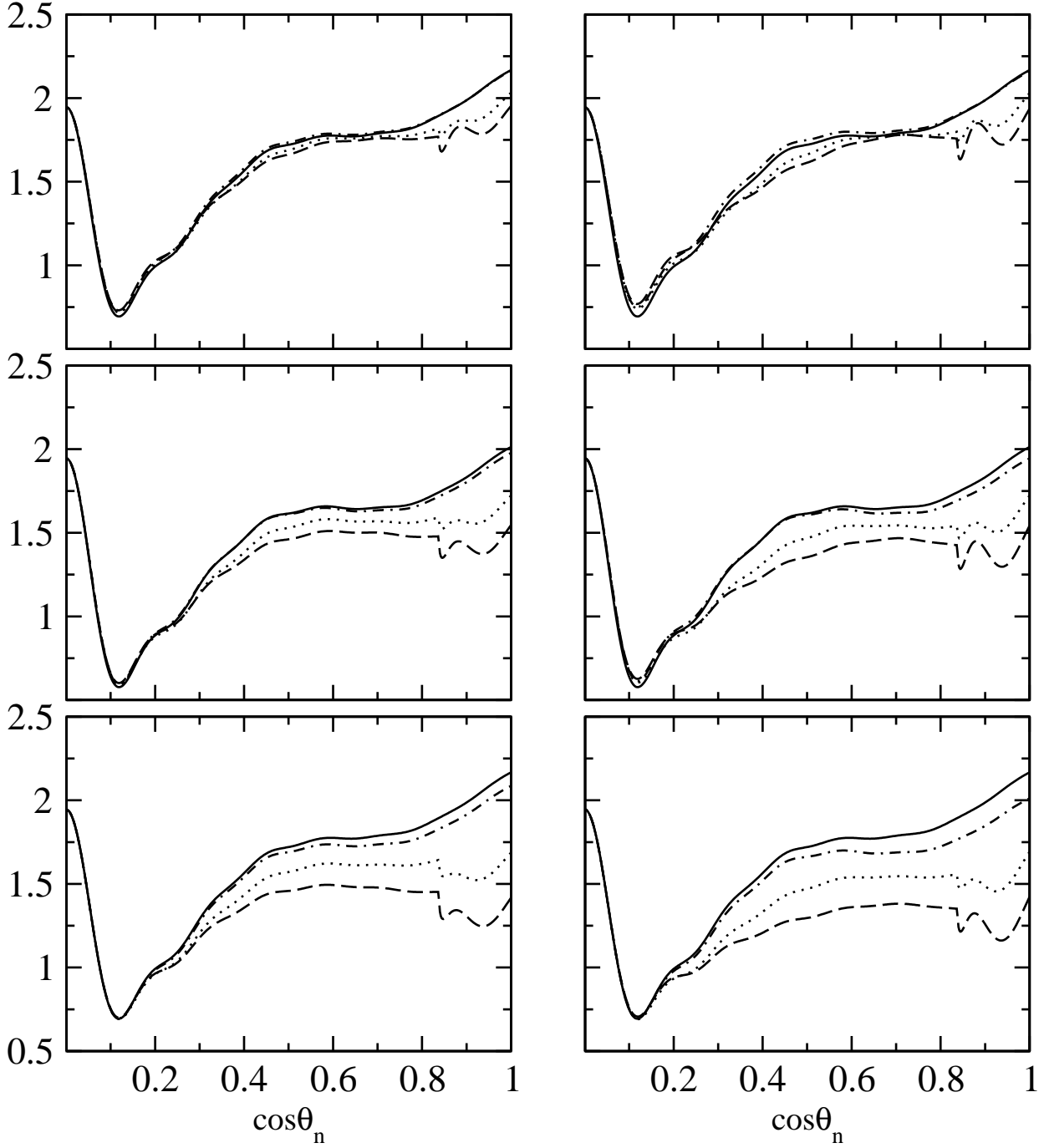


Figure 1: The dependence on $\cos \theta_n$ of the ratios of the multi-GeV and e-like events (or event rates), integrated over the neutrino energy in the interval $E = (2:0 - 10:0)$ GeV, in the cases i) of two-neutrino ν_μ and ν_τ oscillations in vacuum and no ν_e and ν_μ oscillations, $N^2 = N_e^0$ (solid lines), ii) three-neutrino oscillations in vacuum of ν_μ , ν_τ , ν_e and ν_μ , $(N^3 = N_e^3)_{\text{vac}}$ (dash-dotted lines), iii) three-neutrino oscillations of ν_μ , ν_τ and ν_e in the Earth and neutrino mass spectrum with normal hierarchy $(N^3 = N_e^3)_{\text{NH}}$ (dashed lines), or with inverted hierarchy, $(N^3 = N_e^3)_{\text{IH}}$ (dotted lines). The results shown are for $j m_{21}^2 j = 3 \cdot 10^3 \text{ eV}^2$, $\sin^2 2_{23} = 0:36$ (upper panels); $0:50$ (middle panels); $0:64$ (lower panels), and $\sin^2 2_{13} = 0:05$ (left panels); $0:10$ (right panels).

$(N^3 = N_e^3)_{IH}$, for $\sin^2 2_{23} = 0.64; 0.50; 0.36$, $\sin^2 2_{13} = 0.05; 0.10$ and $j m_{31}^2 = 3 \cdot 10^3 \text{ eV}^2$ are shown in Fig. 1.

As $\cos \theta_n$ increases from 0 to 0.2, the neutrino path length in the Earth increases from 0 to $2X^0 = 2R \cos \theta_n = 2550 \text{ km}$. The ν_e ($\bar{\nu}_e$) oscillations, which for $\cos \theta_n < 0.2$ proceed in the Earth essentially as in vacuum, fully develop. For $j m_{31}^2 = 3 \cdot 10^3 \text{ eV}^2$ and $E = 3 \text{ GeV}$, for example, the maximum of the ν_e ($\bar{\nu}_e$) oscillation probability occurs for $\cos \theta_n = 0.1$, or $2X^0 = 1270 \text{ km}$. For $\cos \theta_n < 0.2$ and $j m_{31}^2 = 3 \cdot 10^3 \text{ eV}^2$, the oscillations involving the atmospheric ν_e ($\bar{\nu}_e$; ν_μ ; $\bar{\nu}_\mu$) and ν_e ($\bar{\nu}_e$; ν_τ ; $\bar{\nu}_\tau$) with energies in the multi-GeV range, $E = (2.0 - 10.0) \text{ GeV}$, are suppressed. If $m_{31}^2 > 0$, for instance, the Earth matter effects suppress the antineutrino oscillation probability $P_{2\bar{1}}$, but can enhance the neutrino mixing in matter, or $\sin^2 2_m^0$. However, since the neutrino path in the Earth mantle is relatively short one has $2X^0 E^0 \ll 1$, and correspondingly $P_{2\bar{1}} \ll 1$. Thus, for $\cos \theta_n < 0.2$, all four types of ratios we consider, $N^2 = N_e^0$, $(N^3 = N_e^3)_{vac}$, $(N^3 = N_e^3)_{NH}$ and $(N^3 = N_e^3)_{IH}$, practically coincide and exhibit the same dependence on $\cos \theta_n$: they decrease as $\cos \theta_n$ increases from 0, reaching a minimum at $\cos \theta_n = 0.1$, and begin to rise as $\cos \theta_n$ increases further. This behavior is clearly seen in Figs. 1 and 2.

At $\cos \theta_n > 0.4$, the Earth matter effects in the oscillations of the atmospheric ν_e and $\bar{\nu}_e$, can generate noticeable differences between $N^2 = N_e^0$ (or $(N^3 = N_e^3)_{vac}$) and $(N^3 = N_e^3)_{NH(IH)}$, as well as between $(N^3 = N_e^3)_{NH}$ and $(N^3 = N_e^3)_{IH}$. For $\sin^2 2_{23} = 0.36$ and $\sin^2 2_{13} < 0.05$ (upper left panel in Fig. 1), we have at $\cos \theta_n < 0.3$ (neutrinos crossing only the Earth mantle): $(N^3 = N_e^3)_{NH} = (N^3 = N_e^3)_{IH} = N^2 = N_e^0 = (N^3 = N_e^3)_{vac}$. For the Earth-core-crossing atmospheric neutrinos, $\cos \theta_n > 0.84$, the mantle-core interference effect (or NO LR) suppresses the ratios $(N^3 = N_e^3)_{NH; IH}$ with respect to $N^2 = N_e^0$ (or $(N^3 = N_e^3)_{vac}$): at $\sin^2 2_{13} = 0.10$ the relative averaged difference between $N^2 = N_e^0$ and $(N^3 = N_e^3)_{NH}$ is ⁷ 11%, while the difference between $(N^3 = N_e^3)_{NH}$ and $(N^3 = N_e^3)_{IH}$ is rather small (upper right panel in Fig. 1).

At $\sin^2 2_{23} > 0.50$, the differences between $N^2 = N_e^0$ and $(N^3 = N_e^3)_{NH; IH}$ become noticeable already at $\cos \theta_n > 0.4$. They increase with the increasing of $\sin^2 2_{23}$ and/or $\sin^2 2_{13}$, and are maximal for $\sin^2 2_{23} = 0.64$ and $\sin^2 2_{13} = 0.10$. The dependence on $\sin^2 2_{23}$ is particularly strong. The deviations from the vacuum oscillation ratio $(N^3 = N_e^3)_{vac}$ increase with the increasing of $\cos \theta_n > 0.4$ as well; they are maximal for the Earth-core-crossing neutrinos, $\cos \theta_n > 0.84$.

For $\sin^2 2_{23} = 0.50$ and $\sin^2 2_{13} = 0.05; 0.10$, the relative difference between $N^2 = N_e^0$ and $(N^3 = N_e^3)_{NH}$ in the interval $\cos \theta_n = (0.5 - 0.84)$ is approximately 11%; 13%; for $\sin^2 2_{23} = 0.64$ and $\sin^2 2_{13} = 0.05; 0.10$, it is 18%; 24%. The same differences are larger in the Earth core interval $\cos \theta_n = (0.84 - 1.0)$ due to the mantle-core enhancement (NO LR) [20, 40, 41], reaching on average values of 24%; 27% for $\sin^2 2_{23} = 0.50$ and $\sin^2 2_{13} = 0.05; 0.10$, and 35%; 38% for $\sin^2 2_{23} = 0.64$ and the same two values of $\sin^2 2_{13}$.

For $\sin^2 2_{23} = 0.50$, and $\sin^2 2_{13} = 0.05; 0.10$, the relative difference between $N^2 = N_e^0$ and the ratio $N^3 = N_e^3$ in the case of IH neutrino mass spectrum, $(N^3 = N_e^3)_{IH}$, in the interval $\cos \theta_n = (0.50 - 0.84)$ has a mean value of approximately 6%; 8%, while if $\sin^2 2_{23} = 0.64$ it is approximately 10%; 14%. It is larger in the Earth core bin, $\cos \theta_n = (0.84 - 1.0)$, reaching approximately 25% for $\sin^2 2_{23} = 0.64$ and $\sin^2 2_{13} = 0.10$.

⁷The relative difference of, e.g., $N^2 = N_e^0$ and $(N^3 = N_e^3)_{NH}$ is defined as $(1 - (N^3 = N_e^3)_{NH} / (N^2 = N_e^0))$.

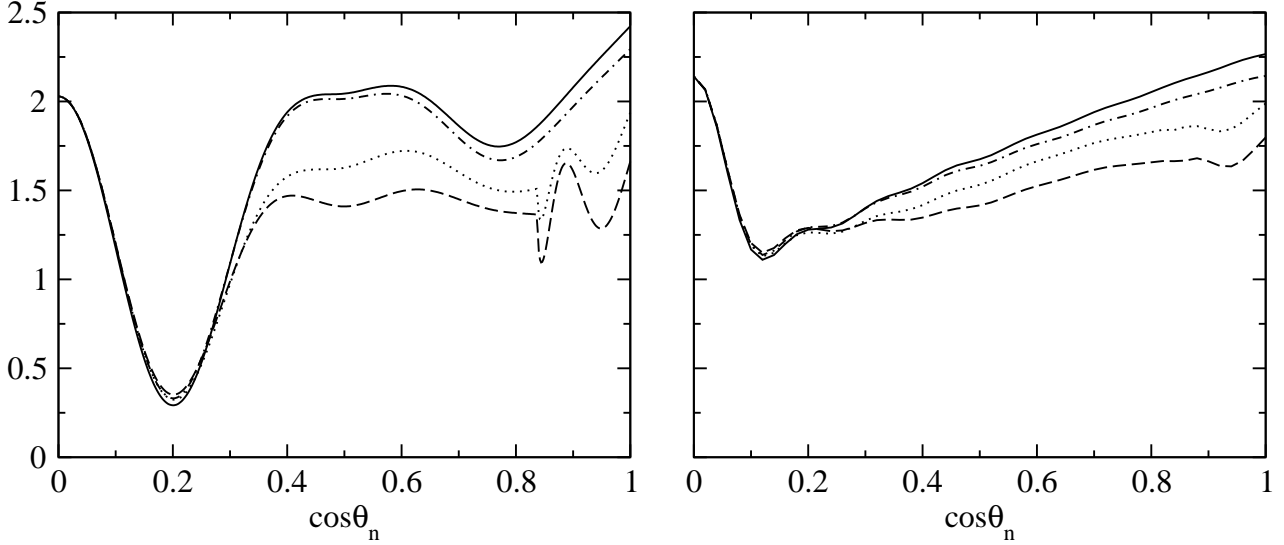


Figure 2: The same as in Fig. 1 but for the ratios of the μ and e like events (or event rates), integrated respectively over the neutrino energy in the intervals $E = (4:0 - 10:0)$ GeV (left panel), and $E = (2:0 - 100:0)$ GeV (right panel), and for $j m_{31}^2 j = 3 \cdot 10^3 \text{ eV}^2$, $\sin^2 \theta_{23} = 0.50$ and $\sin^2 \theta_{13} = 0.10$.

The magnitude of the difference between $N^2 = N_e^0$ and $(N^3 = N_e^3)_{NH (IH)}$ exhibits a relatively strong dependence on the minimal value of the neutrino energy E from the integration interval, E_{min} , and a rather mild dependence on the maximal E in the interval, E_{max} . With the increase of E_{min} , the relative magnitude of the contributions to the energy-integrated event rates of interest, coming from the energy interval in which the matter effects are significant, also increases, leading to larger difference between $N^2 = N_e^0$ and $(N^3 = N_e^3)_{NH (IH)}$. This is illustrated in Fig. 2, where the ratios of interest are shown as functions of $\cos \theta_n$ for $j m_{31}^2 j = 3 \cdot 10^3 \text{ eV}^2$, $\sin^2 \theta_{23} = 0.50$, $\sin^2 \theta_{13} = 0.10$, and i) $E_{min} = 4 \text{ GeV}$, $E_{max} = 10 \text{ GeV}$ (left panel), and ii) $E_{min} = 2 \text{ GeV}$, $E_{max} = 100 \text{ GeV}$ (right panel). Increasing E_{min} (E_{max}) while keeping E_{max} (E_{min}) intact would lead to the decreasing (increasing) of the statistics in the samples of μ like and e like events of interest.

As Fig. 2 illustrates, the relative differences between i) $N^2 = N_e^0$ and $(N^3 = N_e^3)_{NH}$ and ii) $N^2 = N_e^0$ and $(N^3 = N_e^3)_{IH}$, increase noticeably in the interval $\cos \theta_n = (0.40 - 0.65)$ with the increase of E_{min} , being almost constant for $E_{min} = 4 \text{ GeV}$ and reaching the values of approximately 29% and 19%, respectively⁸. For $\cos \theta_n = (0.84 - 1.0)$, the differences under discussion exhibit a characteristic oscillatory pattern. These differences have a completely different behavior as functions of $\cos \theta_n$ if E_{max} is increased to 100 GeV, keeping $E_{min} = 2 \text{ GeV}$ (Fig. 2, right panel): they increase approximately linearly with $\cos \theta_n$, starting from 0 at $\cos \theta_n = 0.25$, and having at $\cos \theta_n = 0.70; 0.84$ the values i) 17% ; 21% and ii) 9% ; 13%, respectively.

In Fig. 3 we show the predictions for the different ratios of μ like and e like event rates we consider, integrated over the neutrino energy in the interval $E = (2 - 10) \text{ GeV}$ and over $\cos \theta_n$ in the interval $\cos \theta_n = (0.4 - 1.0)$, i) as functions of $\sin^2 \theta_{13}$ for $j m_{31}^2 j = 3 \cdot 10^3 \text{ eV}^2$

⁸The relative difference between $(N^3 = N_e^3)_{IH}$ and $(N^3 = N_e^3)_{NH}$ is 12%.

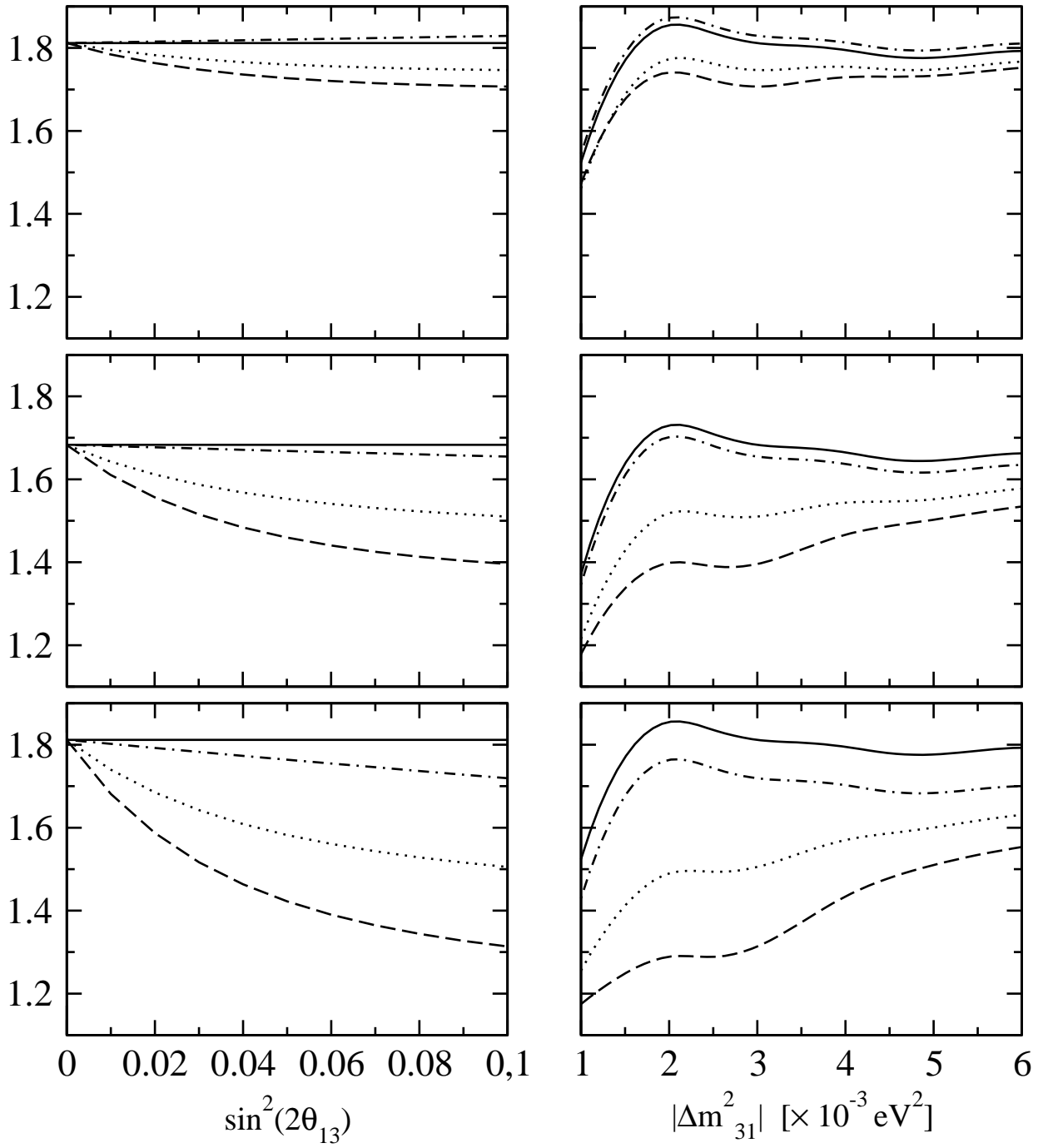


Figure 3: The four different ratios of the multi-GeV and e-like events (or event rates), integrated over the neutrino energy in the interval $E = (2:0 - 10:0)$ GeV and over the Nadir angle in the interval corresponding to $0:40 < \cos \theta_n < 1:0$, as functions i) of $\sin^2 2\theta_{13}$ for $|\Delta m^2_{31}| = 3 \cdot 10^3 \text{ eV}^2$ (left panels), and ii) of $|\Delta m^2_{31}|$ for $\sin^2 2\theta_{13} = 0:10$ (right panels): $N^2 = N_e^0$ (solid lines), $(N^3 = N_e^3)_{\text{vac}}$ (dash-dotted lines), $(N^3 = N_e^3)_{\text{NH}}$ (dashed lines) and $(N^3 = N_e^3)_{\text{IH}}$ (dotted lines). The results shown are obtained for $\sin^2 2\theta_{23} = 0:36$ (upper panels); $0:50$ (middle panels); $0:64$ (lower panels).

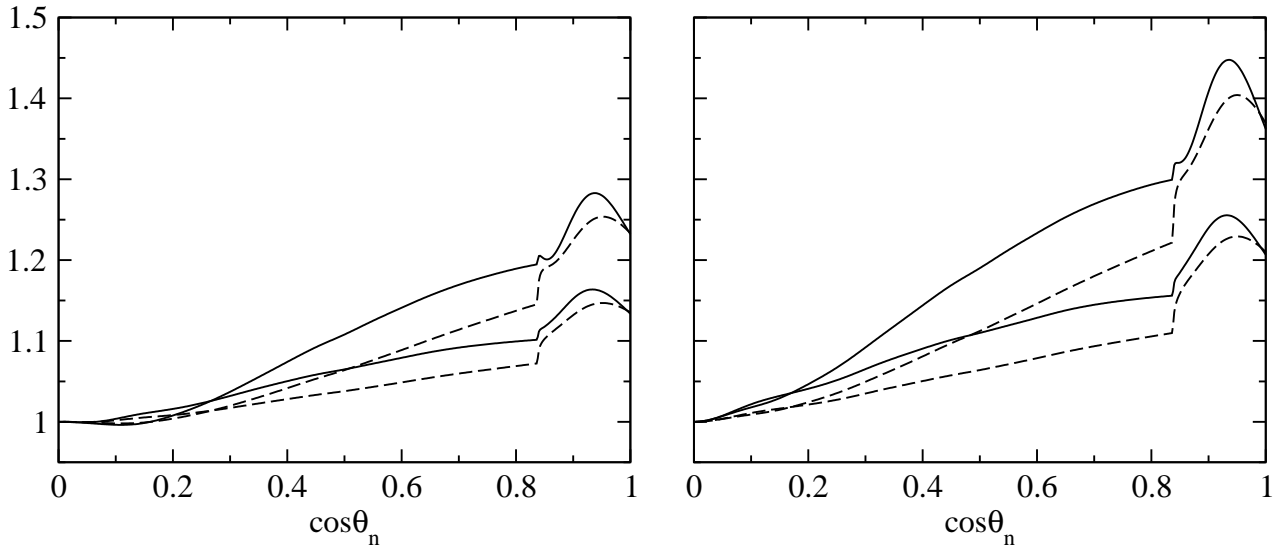


Figure 4: The ratio $N_e^3 = N_e^0$ of e -like multi-GeV events (or event rates), for ν_e and $\bar{\nu}_e$ taking part in 3-neutrino oscillations in the Earth (N_e^3), and ν_e and $\bar{\nu}_e$ not taking part in the oscillations (N_e^0), as a function of $\cos\theta_n$ for $\sin^2 2_{13} = 0.10$ (solid lines); 0.05 (dashed lines), and for neutrino mass spectrum with normal hierarchy (upper solid or dashed lines) and with inverted hierarchy (lower solid or dashed lines). The results shown are for $\sin^2 2_{23} = 0.5$ (left panel); 0.64 (right panel), and for $j m_{31}^2 j = 3 \cdot 10^3 \text{eV}^2$. See text for details.

(left panels), and ii) as functions of $j m_{31}^2 j$ for $\sin^2 2_{13} = 0.10$ (right panel). In each case the results presented are for three values of $\sin^2 2_{23} = 0.36; 0.50; 0.64$. The differences between the ratios of the integrated ν_e -like and $\bar{\nu}_e$ -like event rates of interest, i.e., i) between $N_e^2 = N_e^0$ and $(N_e^3 = N_e^3)_{\text{NH}}$ and ii) between $N_e^2 = N_e^0$ and $(N_e^3 = N_e^3)_{\text{IH}}$, increase rather rapidly as $\sin^2 2_{13}$ increases from 0 to $\sin^2 2_{13} = 0.05$, while the increase is slower in the interval $\sin^2 2_{13} = (0.05 - 0.10)$. At $\sin^2 2_{13} = 0.05$, the relative differences between $N_e^2 = N_e^0$ and i) $(N_e^3 = N_e^3)_{\text{NH}}$ and ii) $(N_e^3 = N_e^3)_{\text{IH}}$ in the case under discussion are respectively 13% and 8% for $\sin^2 2_{23} = 0.50$; for $\sin^2 2_{23} = 0.64$ they are considerably larger, 21% and 13%. If $\sin^2 2_{13} = 0.10$, the same two differences for $\sin^2 2_{23} = 0.50; 0.64$ read 17%; 28% and 10%; 17%, respectively.

It follows from Fig. 3, right panel, that differences between the integrated ratios $N_e^2 = N_e^0$ (or $(N_e^3 = N_e^3)_{\text{vac}}$) and $(N_e^3 = N_e^3)_{\text{NH}}$, and $(N_e^3 = N_e^3)_{\text{IH}}$ and $(N_e^3 = N_e^3)_{\text{NH}}$, are maximal for values of $j m_{31}^2 j$ lying in the interval $(2 - 3) \cdot 10^3 \text{eV}^2$, which are favored by the current atmospheric neutrino data.

In Figs. 4 and 5 we present results just for the multi-GeV e -like event rate. The Earth matter effects are largest in the oscillations of the atmospheric ν_e or $\bar{\nu}_e$. The dependence of the ratio $N_e^3 = N_e^0$, N_e^3 and N_e^0 being the numbers of multi-GeV e -like events (or event rates) predicted in the cases of 3-oscillations of ν_e , $\bar{\nu}_e$, and of absence of oscillations ($\sin^2 2_{13} = 0$), on $\cos\theta_n$ is shown in Fig. 4 for $\sin^2 2_{23} = 0.50; 0.64$ and for $\sin^2 2_{13} = 0.05; 0.10$. The deviation of $N_e^3 = N_e^0$ from 1 would signal that ν_e and $\bar{\nu}_e$ take part in oscillations and that $\sin^2 2_{13} \neq 0$. We can have $N_e^3 = N_e^0 > 1$ only if a substantial fraction of the atmospheric (ν_e or $\bar{\nu}_e$) oscillate into ν_e ($\bar{\nu}_e$). As Fig. 4 shows, the ratio $N_e^3 = N_e^0$ increases with the

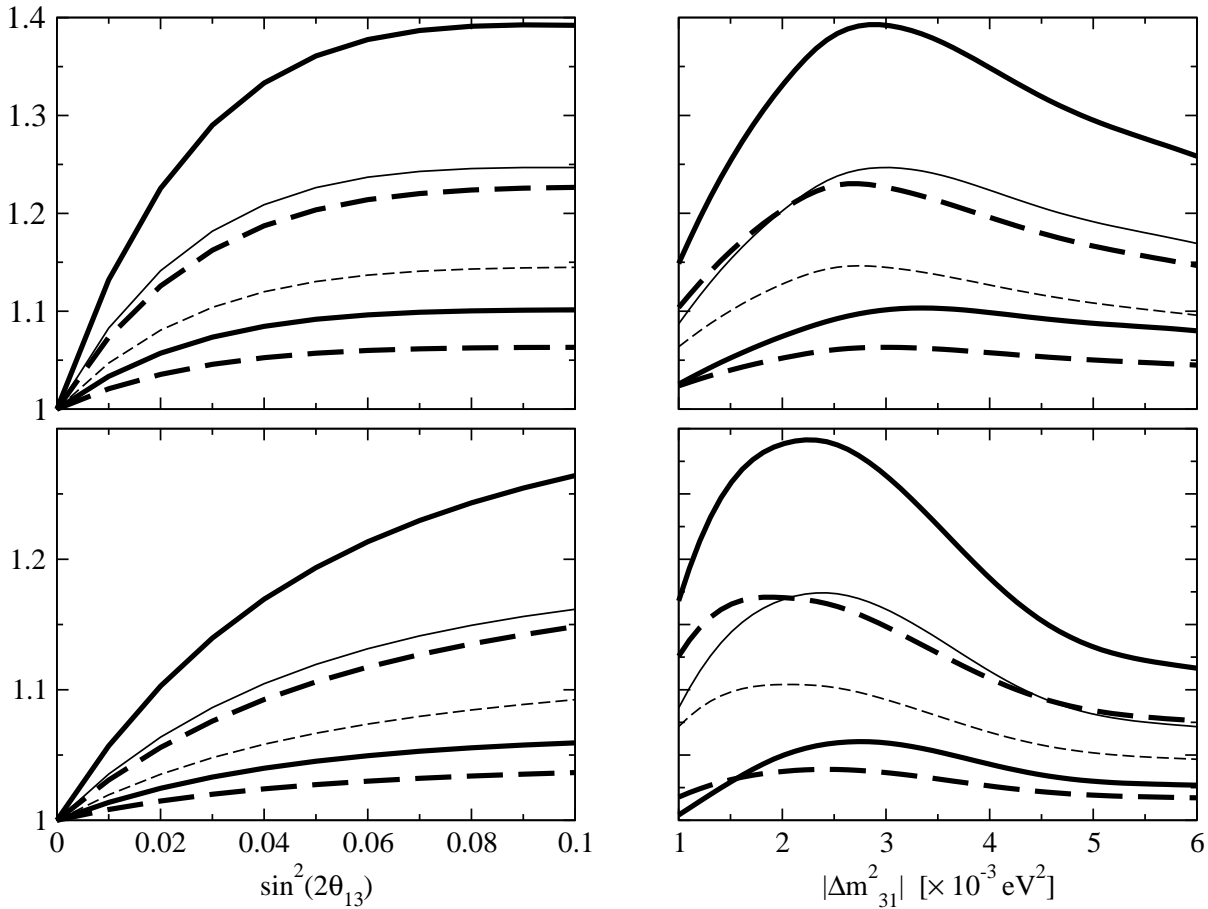


Figure 5: The dependence of the ratio $N_e^3 = N_e^0$ i) on $\sin^2 \theta_{13}$ for $\cos \theta_n = 1.0$ (upper panels), and ii) on $|\Delta m_{31}^2|$ for $\sin^2 \theta_{13} = 0.10$ (right panels), in the cases of neutrino mass spectrum with normal hierarchy (solid lines) and inverted hierarchy (dashed lines). In this figure N_e^3 and N_e^0 are the multi-GeV e -like events (or event rates) for e and e taking part in 3-neutrino oscillations in the Earth and e and e not taking part in the oscillations, respectively, integrated over the Nadir angle θ_n in the intervals corresponding to a) $0.84 < \cos \theta_n < 1.0$ - neutrinos crossing the Earth core (upper panels), and b) $0.40 < \cos \theta_n < 1.0$ (lower panels). The results shown are for $\sin^2 \theta_{23} = 0.36$ (lower doubly thick solid or dashed lines); 0.50 (middle thin solid or dashed lines); 0.64 (upper doubly thick solid or dashed lines).

increasing of $\cos \theta_n$ and can be significantly greater than 1 for $\cos \theta_n > 0.4$. At $\cos \theta_n = 0.8$, for instance, we have for $\sin^2 \theta_{23} = 0.50$ and $\sin^2 \theta_{13} = 0.05; 0.10$ in the case of NH neutrino mass spectrum $(N_e^3 = N_e^0)_{NH} = 1.14; 1.19$, while for $\sin^2 \theta_{23} = 0.64$ one finds $(N_e^3 = N_e^0)_{NH} = 1.21; 1.29$. For IH neutrino mass spectrum the ratio of interest, $(N_e^3 = N_e^0)_{IH}$, is smaller and the corresponding values read: $(N_e^3 = N_e^0)_{IH} = 1.07; 1.10$ and $(N_e^3 = N_e^0)_{IH} = 1.11; 1.15$, respectively. For the Earth-core-crossing neutrinos both $(N_e^3 = N_e^0)_{NH}$ and $(N_e^3 = N_e^0)_{IH}$ are larger due to the NO LR effect, and for $\sin^2 \theta_{23} = 0.64$ and $\sin^2 \theta_{13} = 0.10$ reach the values $(N_e^3 = N_e^0)_{NH} = 1.45$ and $(N_e^3 = N_e^0)_{IH} = 1.26$.

For given $\sin^2 \theta_{23}$ and $\sin^2 \theta_{13}$, the maximum of the ratio of the multi-GeV e -like

event rates of interest N_e^3 and N_e^0 , integrated over θ_n in the intervals corresponding to a) $\cos \theta_n = (0.84 \quad 1.0)$ (Earth core bin) and b) $\cos \theta_n = (0.40 \quad 1.0)$, occurs again for values of $j m_{31}^2 j = (2 \quad 3) \cdot 10^3 \text{ eV}^2$ (Fig. 5, right panels), favored by the existing atmospheric neutrino data. For $j m_{31}^2 j = 3 \cdot 10^3 \text{ eV}^2$, $\sin^2_{13} = (0.05 \quad 0.10)$ and $\sin^2_{23} = 0.64$, the two types of θ_n integrated ratios can be as large as: case a) $(N_e^3 = N_e^0)_{NH (IH)} = 1.36 \quad 1.39 (1.20 \quad 1.23)$, and case b) $(N_e^3 = N_e^0)_{NH (IH)} = 1.19 \quad 1.26 (1.11 \quad 1.15)$ (Fig. 5, left and right panels).

4 Conclusions

In the present article we have studied the possibility to obtain evidences for Earth matter enhanced 3-neutrino oscillations of the atmospheric neutrinos involving, in particular, the ν_e (or $\bar{\nu}_e$), from the analysis of the μ -like and e -like multi-GeV event data accumulated by the SK experiment, or that can be provided by future water-Cherenkov detectors. Such evidences would give also important quantitative information on the values of \sin^2_{13} and \sin^2_{23} and on the sign of $m_A^2 = m_{31}^2$. We have considered 3-neutrino oscillations of the atmospheric ν_μ , ν_e and $\bar{\nu}_e$, assuming that the inequality $m^2 = m_{21}^2 \quad j m_A^2 j = j m_{31}^2 j$ holds, as is suggested by the current solar and atmospheric neutrino data. Depending on the sign of m_{31}^2 , the Earth matter effects in this case can enhance either the $\nu_\mu \rightarrow \nu_e$ and $\bar{\nu}_\mu \rightarrow \bar{\nu}_e$, or the $\nu_\mu \rightarrow \bar{\nu}_e$ and $\bar{\nu}_\mu \rightarrow \nu_e$ transitions if $\sin^2_{13} \neq 0$. The effects of the enhancement can be substantial for $\sin^2_{13} > 0.01$ and $\sin^2_{23} > 0.50$. They are largest in the multi-GeV e -like and μ -like samples of events and for atmospheric neutrinos with relatively large path length in the Earth, crossing deeply the mantle or the mantle and the core, i.e., for $\cos \theta_n > 0.4$, where θ_n is the Nadir angle characterizing the neutrino trajectory in the Earth.

As observables which are particularly sensitive to the Earth matter effects, and thus to the values of \sin^2_{13} and \sin^2_{23} , and to the sign of m_{31}^2 , we have considered the Nadir-angle distributions of the ratios $N^3 = N_e^3$ and $N_e^3 = N_e^0$, where N^3 and N_e^3 are the multi-GeV μ -like and e -like numbers of events (or event rates) in the case of 3-oscillations of the atmospheric ν_μ , ν_e and $\bar{\nu}_e$, and N_e^0 is the number of e -like events in the case of absence of oscillations ($\sin^2_{13} = 0$). As is well-known, the ratio of the energy and Nadir angle integrated μ -like and e -like events, $N = N_e$, has been measured with a relatively high precision by the SK experiment [3].

We have obtained predictions for the Nadir-angle distributions of $N^3 = N_e^3$ and of $N_e^3 = N_e^0$ both for neutrino mass spectra with normal ($m_{31}^2 > 0$) and inverted ($m_{31}^2 < 0$) hierarchy, $(N^3 = N_e^3)_{NH}$, $(N^3 = N_e^3)_{IH}$, $(N_e^3 = N_e^0)_{NH}$ and $(N_e^3 = N_e^0)_{IH}$, and for $\sin^2_{23} = 0.64; 0.50; 0.36$. We compared the latter with the predicted Nadir-angle distributions i) of the ratio $N = N_e$ for the case the 3-neutrino oscillations taking place in vacuum, $(N^3 = N_e^3)_{vac}$, and ii) of the ratio $N^2 = N_e^0$, the predicted number of μ -like and e -like events in the case of 2-neutrino $\nu_\mu \rightarrow \nu_\tau$ and $\bar{\nu}_\mu \rightarrow \bar{\nu}_\tau$ oscillations of the atmospheric ν_μ and $\bar{\nu}_\mu$, and ν_e and $\bar{\nu}_e$ not taking part in the oscillations ($\sin^2_{13} = 0$). The dependence of the Nadir angle distributions of $(N^3 = N_e^3)_{NH}$, $(N^3 = N_e^3)_{IH}$, $(N_e^3 = N_e^0)_{vac}$ and $N^2 = N_e^0$ on the minimal and maximal neutrino energies in the energy integration interval has also been studied. Predictions for these four different types of ratios of the suitably integrated over θ_n Nadir angle distributions of the μ -like and e -like multi-GeV events were also derived.

Our results are presented graphically in Figs. 1–5. We find that for $\sin^2 2_{23} = 0.50$ and $\sin^2 2_{13} = 0.05$, the relative difference between $N^2 = N_e^0$ and $(N^3 = N_e^3)_{NH}$ in the interval $\cos \theta_n = (0.5 \quad 0.84)$ is approximately 11%. If $\sin^2 2_{23} = 0.64$ and $\sin^2 2_{13} = 0.10$, the same difference is approximately 24% (Fig. 1). The relative difference between $N^2 = N_e^0$ and $(N^3 = N_e^3)_{NH}$ is larger in the Earth core interval $\cos \theta_n = (0.84 \quad 1.0)$ due to the mantle-core enhancement (NOLR) [20, 40, 41], reaching on average values of 24% for $\sin^2 2_{23} = 0.50$ and $\sin^2 2_{13} = 0.05$, and of 38% for $\sin^2 2_{23} = 0.64$ and $\sin^2 2_{13} = 0.10$ (Fig. 1).

In the case of neutrino mass spectrum with inverted hierarchy, the relative difference between $N^2 = N_e^0$ and $(N^3 = N_e^3)_{IH}$ in the interval $\cos \theta_n = (0.50 \quad 0.84)$ has a mean value of approximately 14%, for $\sin^2 2_{23} = 0.64$ and $\sin^2 2_{13} = 0.10$. It reaches approximately 25% in the Earth core bin, $\cos \theta_n = (0.84 \quad 1.0)$, for these values of $\sin^2 2_{23}$ and $\sin^2 2_{13}$ (Fig. 1).

The magnitude of the difference between $N^2 = N_e^0$ and $(N^3 = N_e^3)_{NH(IH)}$ exhibits a relatively strong dependence on the minimal value of the neutrino energy E from the integration interval, E_{min} , and a rather mild dependence on the maximal E in the integration interval, E_{max} (Fig. 2). Increasing E_{min} from 2 GeV to 4 GeV and keeping $E_{max} = 10$ GeV, leads for $j m_{31}^2 = 3 \cdot 10^3 \text{ eV}^2$, $\sin^2 2_{23} = 0.50$ and $\sin^2 2_{13} = 0.10$ to a considerably larger relative difference between $N^2 = N_e^0$ and $(N^3 = N_e^3)_{NH(IH)}$ in the interval $\cos \theta_n = (0.40 \quad 0.65)$, which reaches approximately 29% (19%) (Fig. 2). This difference is larger also in the Earth core bin, $\cos \theta_n = (0.84 \quad 1.0)$. We have also found that the differences between the Nadir angle and energy integrated ratios $N^2 = N_e^0$ (or $(N^3 = N_e^3)_{vac}$) and $(N^3 = N_e^3)_{NH}$, and $(N^3 = N_e^3)_{IH}$ and $(N^3 = N_e^3)_{NH}$, are maximal for values of $j m_{31}^2$ lying in the interval $(2 \quad 3) \cdot 10^3 \text{ eV}^2$, which are favored by the current atmospheric neutrino data (Fig. 3). The same conclusion is valid for the integrated ratio of electron-like events $N_e^3 = N_e^0$ (Fig. 5).

We have also shown that in the case of the 3-neutrino oscillations of the atmospheric neutrinos considered, the ratio $N_e^3 = N_e^0$ increases with the increasing of $\cos \theta_n$ and can be significantly greater than 1 for $\cos \theta_n > 0.4$. At $\cos \theta_n = 0.8$, for instance, we have for $\sin^2 2_{23} = 0.50$ and $\sin^2 2_{13} = 0.10$ in the case of NH neutrino mass spectrum $(N_e^3 = N_e^0)_{NH} = 1.19$, while for $\sin^2 2_{23} = 0.64$ one finds $(N_e^3 = N_e^0)_{NH} = 1.29$ (Fig. 4). For IH neutrino mass spectrum the ratio of interest, $(N_e^3 = N_e^0)_{IH}$, is smaller: $(N_e^3 = N_e^0)_{IH} = 1.10$ and 1.15. For the Earth-core-crossing neutrinos both $(N_e^3 = N_e^0)_{NH}$ and $(N_e^3 = N_e^0)_{IH}$ are enhanced due to the NOLR effect, and for $\sin^2 2_{23} = 0.64$ and $\sin^2 2_{13} = 0.10$ reach the values $(N_e^3 = N_e^0)_{NH} = 1.45$ and $(N_e^3 = N_e^0)_{IH} = 1.26$ (Fig. 4).

It follows from our results that the Earth matter effects in the Nadir angle distribution of the ratio of the multi-GeV electron-like and electron-like atmospheric neutrino events (or event rates), measured in the Super-Kamiokande (or any future water-Cherenkov) experiment, might be observable if the atmospheric neutrinos, including the ν_e and $\bar{\nu}_e$, take part in 3-neutrino oscillations and $\sin^2 2_{13}$ and $\sin^2 2_{23}$ are sufficiently large. The observation of relatively large Earth matter effects (20%–30%) at $\cos \theta_n > 0.4$ would clearly indicate that $\sin^2 2_{13} > 0.01$, $\sin^2 2_{23} > 0.50$, and would suggest that the neutrino mass spectrum is with normal hierarchy, $m_{31}^2 > 0$. However, distinguishing statistically between the neutrino mass spectrum with normal and inverted hierarchy requires a high precision measurement of the Nadir angle distribution of the multi-GeV ratio $N = N_e$ and is a rather challenging task.

Acknowledgements

This work is supported in part by the Italian M IUR and INFN under the programs "Fenomenologia delle Interazioni Fondamentali" and "Fisica Astroparticellare", by the U.S. National Science Foundation under Grant No. PHY 99-07949 (S.T.P.), by the Spanish Grant FPA 2002-00612 of the MCT (J.B. and S.P.-R.) and by the Spanish MEC for a FPU fellowship (S.P.-R.). S.T.P. would like to thank the organizers of the Program on "Neutrinos: Data, Cosmology and the Planck Scale" at KITP, Univ. of California at Santa Barbara, where part of the work on the present study was done, for kind hospitality, and M. Freund for discussions at the initial stage of this work. S.P.-R. would like to thank the Elementary Particle Physics Sector of SISSA, Trieste, Italy, for kind hospitality during part of this study.

References

- [1] B. T. Cleveland et al., *Astrophys. J.* 496 (1998) 505; Y. Fukuda et al., *Phys. Rev. Lett.* 77 (1996) 1683; V. Gavrin, *Nucl. Phys. Proc. Suppl.* 91 (2001) 36; W. Hampel et al., *Phys. Lett. B* 447 (1999) 127; M. Ahlmann et al., *Phys. Lett. B* 490 (2000) 16.
- [2] Super-Kamiokande Collaboration, Y. Fukuda et al., *Phys. Rev. Lett.* 86 (2001) 5651 and 5656.
- [3] Super-Kamiokande Collaboration, M. Shiozawa, talk given at the Int. Conf. on Neutrino Physics and Astrophysics "Neutrino'02", May 25 - 30, 2002, Munich, Germany.
- [4] SNO Collaboration, Q. R. Ahmad et al., *Phys. Rev. Lett.* 87 (2001) 071301.
- [5] SNO Collaboration, Q. R. Ahmad et al., *Phys. Rev. Lett.* 89 (2002) 011302 and 011301.
- [6] KamLAND Collaboration, K. Eguchi et al., *Phys. Rev. Lett.* 90 (2003) 021802.
- [7] B. Pontecorvo, Chalk River Lab. report PD 205, 1946; *Zh. Eksp. Teor. Fiz.* 53 (1967) 1717.
- [8] R. Davis, D. S. Harmer and K. C. Hoffman, *Phys. Rev. Lett.* 20, 1205 (1968); *Acta Physica Acad. Sci. Hung.* 29 Suppl. 4, 371 (1970); R. Davis, Proc. of the "Neutrino '72" Int. Conference, Balatonfured, Hungary, June 1972 (eds. A. Frenkel and G. Marx, OM KDK-TECHNOINFORM, Budapest, 1972), p. 5.
- [9] S. M. Bilenky, C. Giunti and W. Grimus, *Prog. Part. Nucl. Phys.* 43 (1999) 1.
- [10] B. Pontecorvo, *Zh. Eksp. Teor. Fiz.* 33 (1957) 549 and 34 (1958) 247; Z. Maki, M. Nakagawa and S. Sakata, *Prog. Theor. Phys.* 28 (1962) 870.
- [11] S. M. Bilenky et al., *Phys. Lett. B* 94 (1980) 495; M. Doi et al., *Phys. Lett. B* 102 (1981) 323; J. Bernabeu and P. Pascual, *Nucl. Phys. B* 228 (1983) 21; P. Langacker et al., *Nucl. Phys. B* 282 (1987) 589.
- [12] S. M. Bilenky and S. T. Petcov, *Rev. Mod. Phys.* 59 (1987) 671.

- [13] M. Apollonio et al., Phys. Lett. B 466 (1999) 415.
- [14] F. Boehm et al., Phys. Rev. Lett. 84 (2000) 3764 and Phys. Rev. D 62 (2000) 072002.
- [15] G. L. Fogli et al., Phys. Rev. D 67 (2003) 073002.
- [16] V. Barger and D. Marfatia, Phys. Lett. B 555 (2003) 144; M. Maltoni, T. Schwetz, and J. W. F. Valle, hep-ph/0212129; A. Bandyopadhyay et al., Phys. Lett. B 559 (2003) 121; J. N. Bahcall, M. C. Gonzalez-Garcia and C. Pena-Garay, JHEP 0302 (2003) 009; H. Nunokawa, W. J. C. Teves, and R. Zukanovich Funchal, hep-ph/0212202; P. Aliani et al., hep-ph/0212212; P. C. de Holanda and A. Y. Smirnov, JCAP 0302 (2003) 001; A. B. Balantekin and H. Yuksel, J. Phys. G 29 (2003) 665.
- [17] G. L. Fogli et al., Phys. Rev. D 66 (2002) 093008
- [18] S. M. Bilenky, D. Nicolopoulos and S. T. Petcov, Phys. Lett. B 538 (2002) 77.
- [19] A. DeRujula et al., Nucl. Phys. B 168 (1980) 54.
- [20] S. T. Petcov, Phys. Lett. B 434 (1998) 321, (E) ibid. B 444 (1998) 584.
- [21] S. T. Petcov, Nucl. Phys. B (Proc. Suppl.) 77 (1999) 93, hep-ph/9809587, hep-ph/9811205 and hep-ph/9907216.
- [22] M. V. Chizhov, M. Maris and S. T. Petcov, hep-ph/9810501.
- [23] A. DeRujula, M. B. Gavela and P. Hernandez, Nucl. Phys. B 547, 21 (1999); V. Barger et al., Phys. Rev. D 62, 013004 (2000).
- [24] M. Freund et al., Nucl. Phys. B 578 (2000) 27.
- [25] M. C. Baruls, G. Barenboim and J. Bernabeu, Phys. Lett. B 513, 391 (2001).
- [26] J. Bernabeu and S. Palmares-Ruiz, hep-ph/0112002, and Nucl. Phys. Proc. Suppl. 110, 339 (2002), hep-ph/0201090.
- [27] P. I. Krastev and S. T. Petcov, Phys. Lett. B 205 (1988) 84.
- [28] J. Arifino and J. Sato, Phys. Rev. D 55 (1997) 1653; J. Bernabeu, Proc. W IN '99, World Scientific (2000), p. 227, hep-ph/9904474.
- [29] K. Dick et al., Nucl. Phys. B 562 (1999) 29.
- [30] J. Bernabeu and M. C. Baruls, Nucl. Phys. Proc. Suppl. 87 (2000) 315, hep-ph/0003299.
- [31] S. M. Bilenky, S. Pascoli and S. T. Petcov, Phys. Rev. D 64 (2001) 053010; S. Pascoli and S. T. Petcov, Phys. Lett. B 544 (2002) 239; S. Pascoli, S. T. Petcov and W. Rodejohann, Phys. Lett. B 558 (2003) 141.
- [32] L. Wolfenstein, Phys. Rev. D 17, 2369 (1978), and ibid. D 20, 2634 (1979).

- [33] V. Barger et al., *Phys. Rev. D* 22, 2718 (1980).
- [34] S. P. Mikheyev and A. Yu. Smirnov, *Yad. Fiz.* 42, 1441 (1985) [*Sov. J. Nucl. Phys.* 42, 913 (1985)].
- [35] S. M. Bilenky et al., *Phys. Lett. B* 465 (1999) 193.
- [36] D. Michael (MINOS Collaboration), Talk at the Int. Conf. on Neutrino Physics and Astrophysics "Neutrino'02", May 25 – 30, 2002, Munich, Germany.
- [37] M. Spiro, Summary talk at the Int. Conf. on Neutrino Physics and Astrophysics "Neutrino'02", May 25 – 30, 2002, Munich, Germany.
- [38] V. Barger, D. Marfatia and K. Whisnant, *Phys. Lett. B* 560 (2003) 75; P. Huber, M. Lindner and W. Winter, *Nucl. Phys. B* 654 (2003) 3
- [39] S. T. Petcov and M. Piai, *Phys. Lett. B* 533 (2002) 94.
- [40] M. V. Chizhov and S. T. Petcov, *Phys. Rev. Lett.* 83 (1999) 1096.
- [41] M. V. Chizhov and S. T. Petcov, *Phys. Rev. D* 63 (2001) 073003.
- [42] J. Bernabeu, S. Palmares-Ruiz, A. Perez and S. T. Petcov, *Phys. Lett. B* 531, 90 (2002)
- [43] M. C. Gonzalez-Garcia and M. Maltoni, *Eur. Phys. J. C* 26 (2003) 417
- [44] S. T. Petcov, *Phys. Lett. B* 214, 259 (1988).
- [45] M. Honda et al., *Phys. Rev. D* 52, 4985 (1995).
- [46] V. Agraal et al., *Phys. Rev. D* 53, 1314 (1996).
- [47] G. Fiorentini, V. A. Naumov and F. L. Villante, *Phys. Lett. B* 578 (2000) 27.
- [48] F. D. Stacey, *Physics of the Earth*, 2nd edition, John Wiley and Sons, London, New York, 1977.
- [49] A. D. Dziewonski and D. L. Anderson, *Physics of the Earth and Planetary Interiors* 25, 297 (1981).
- [50] M. Maris and S. T. Petcov, *Phys. Rev. D* 56 (1997) 7444.
- [51] M. Maris, Q. Y. Liu and S. T. Petcov, study performed in November – December of 1996 (unpublished).
- [52] R. Jeanloz, *Annu. Rev. Earth Planet. Sci.* 18, 356 (1990); C. J. Allegre et al., *Earth Planet. Sci. Lett.* 134, 515 (1995); W. F. McDonough and S.-s. Sun, *Chemical Geology* 120, 223 (1995).
- [53] M. Gluck, E. Reya and A. Vogt, *Z. Phys. C* 67 (1995) 433.